Chapter 3

Applications to Radiotherapy Using Three Different Dosimetric Tools: MAGIC-*f* Gel, PENELOPE Simulation Code and Treatment Planning System

Thatiane Alves Pianoschi and Mirko Salomón Alva-Sánchez

Additional information is available at the end of the chapter

http://dx.doi.org/10.5772/56349

1. Introduction

Electron beams are widely used in radiotherapy with superior advantages in the irradiation of near-surface targets compared to photon beams, due to their characteristic therapeutic range and the plateau of the dose, finding between 80% and 90% of the maximum dose on central axis, and steep falloff of the dose with depth, characteristics that not exist in photon beams.

Thus, the electron beams are an important therapeutic modality for superficial treatments involving: skin and lip cancer, cancer of the chest wall and neck (after surgery and for recurrent cancers), upper respiratory and digestive tract lesions from 1 to 5 cm depth and reinforcement in the treatment of lymph nodes, scars from surgeries and residual tumors [1].

The main dosimetric parameter used for planning in radiotherapy with electron beams is obtained through the curves of percentage depth dose (PDD) [2]. From the PDD one can determine the maximum, practical and therapeutic range of the beam, the depth of maximum dose and depths that receive 90 % and 50% of the maximum dose.

Measurements of the dosimetric parameters with electron beam are more complex due to beam characteristics, especially the high dose gradient, which is present when the dose suffers a sharp drop after the build-up region. Standard dosimeters like ionization chamber, TLD and film do not have a high resolution, low energy dependence and the possibility of use with high dose gradient. Thus, the choice of the dosimeter for this type of beam is primordial.

The dosimetry gel have a high resolution, with atomic number equivalent to water and the possibility of providing measurement of high dose gradients in three-dimensions. Amongst the gel dosimeters, the MAGIC-*f* gel has been showed great concordance with the reference dosimeters.

After being exposed to ionizing radiation, the compounds of the MAGIC-*f* gel undergo a polymer reaction, that results in a chain of polymers that is completed after some days. The formation of the polymeric chain can be co-related with the absorbed dose, that can be seen on magnetic resonance images and through this imaging a three dimensional dose in target volume can be computed.

Another effective dosimetric tool for the study of this beam is the Monte Carlo simulation codes, that offers a convenient alternative compared to experimental methods, with advantage of providing detailed studies, and in different conditions that involve experimental procedures which are lengthy, complex and expensive [3]. The use of PENELOPE-Monte Carlo simulation code to simulate phenomena of attenuation of the dose radiation and dose deposition has been on an increase. The reliability of the results found by this code is directly related to the accuracy of transport models and the cross section libraries of the particles transported [4].

This chapter will be discuss the application of the two dosimetric tools, the MAGIC-*f* gel dosimeter and PENELOPE-Monte Carlo simulation code with high spatial resolution for determination of tridimensional dose distributions in target volumes for electron beams.

2. MAGIC-*f* gel dosimeter

Dosimeters based on polymeric gels are compounds that polymerize when subjected to radiation, this polymerization is related with the absorbed dose. Due to this property, these dosimeters have the ability to store information of the dose distributions in three-dimensios (3D). This is an advantage compared to other dosimeters providing only dose in a point or two-dimensional, as ionization chambers and films, respectively. This advantage is particularly important for the new technologies related with the radiation, where a significant incidence of high dose gradients is recorded.

The proposed sensitivity of gels to radiation was suggested by Stein and Day in 1950 when it was shown that the gels alter color depending on the absorbed dose [5]. In 1957 Andrews and colleagues studied the dose distribution and measurements of the pH of sensitive gels by spectroscopy [6]. The use of these gels as a dosimeter began with Gore and colleagues in 1984 when it was investigated the Fricke gels, initially studied by Fricke and Morse in 1927, based on the principle of oxidation, and recorded the relaxation properties in nuclear magnetic resonance (NMR) and showed that the concentration of ferric ions could be quantified by this technique [7].

Besides the research on Fricke gel, the studies with other gel dosimeters, polymer dosimeters as: BANANA (bis acrylamide and agarose nitrous oxide) [8], BANG (bis acrylamide gel nitrous oxide) [9] and PAG (acrylamide polymer gelatine) were started [10].

In polymeric dosimeters, monomeric compounds of the dosimeters are immersed in a gelatinous matrix, aqueous polymer suffer a reaction to the absorbed dose, resulting in a polymer gel matrix. This formation of radio-induced products changes the NMR relaxation properties, which can be related to the absorbed dose deposition, thus presenting a potential dosimeter for clinical dosimetry in 3D. However, the polymerization can be inhibited due to presence of oxygen, hence hypoxic conditions are required for its manufacture. To solve this problem Fong et al [11] created a new polymer gel, MAGIC (methacrylic and ascorbic acid in gelatin initiated by copper), formed by the combination of methacrylate-based materials, ascorbic acid and salt copper. The oxygen uptake is given by ascobato-copper complex, which allows the preparation of polymeric gels in normal atmospheric conditions in 2001[12-14]. Another problem presented by the polymer gels was the melting of the samples when stored at room temperature causing loss of information about dose distribution thereby restricting its use. In 2008, Fernandes and colleagues [15] solved this problem by adding formaldehyde to the original formulation of the MAGIC increasing its melting point to 69 ° C, and named the new gel MAGIC-f.

3. PENELOPE simulation code

The Monte Carlo method is a technique that uses the sampling of random numbers and statistical methods to find solutions to mathematical or physical problems [16]. In the Monte Carlo simulation (SMC) of radiation transport, the history of a particle is described as a probabilistic sequence of interactions when the particle changes its direction of movement, losing a part or all its energy, and occasionally generating a secondary particle [4].

Among the SMC codes used to simulate the interaction of radiation with matter, EGS [17], MCNP [18] and, more recently, PENELOPE [19] and GEANT [20] have been applied to radiology. The quality of the results provided by different simulation codes is directly linked with the accuracy of the transport model and implemented by libraries that contain the data associated with the cross section of particles transported [4]. The transport algorithm implemented by PENELOPE [3], led to its extensive use in radiotherapy [21-27].

Thus, the Monte Carlo simulation code PENELOPE, freely distributed by the Nuclear Energy Agency (NEA) is used to simulate the transport of electrons, positrons and photons in a complex geometry and an arbitrary material. The subroutines of FORTRAN code are organized into four basic files: PENELOPE.f containing the subroutines of transport of particles, PENGEOM.f containing subroutines geometry; PENVARED.f containing the subroutines that perform the methods of reducing variations and TIMER.f, which manages the simulation time. Besides these files, the code has a database with the characteristics of various materials of interest in radiological physics [28] cross section libraries and other quantities necessary for the transport of particles. One of the main advantages of using the code SMC is the use of recent cross-section libraries, EPDL97 [19].

The algorithm uses a simulation model PENELOPE combining numerical data and analytical cross section for the different types of interactions. It is applied from 1 keV energy to approximately 1 GeV where a detailed transport of photons is simulated by a

conventional method. The simulation of electrons and positrons is made by means of a mixed algorithm because the latter undergo a large number of iterations before being effectively absorbed by the medium, resulting in small energy losses making it impractical to use a detailed method (or class I) for the transport of these particles.

Thus, for electrons and positrons, the PENELOPE code differs from other simulation codes by using a mixed algorithm (or class II), which implements two simulation models: a detailed, strong events, defined as the deflection angle (angle scattering) or loss of energy above a preset value, and condensed to weak interactions, with angular deflection (scattering angle) or loss of energy lower than the pre-set values. The condensed interactions are described by an approximation of multiple scattering, which consists in transforming a large number of weak interactions in a single artificial event. The multiple scattering theory algorithms implemented in the simulation is made condensed approximations and can lead to systematic errors assigned to the dependence of the simulation parameters that control the transport.

4. Treatment planning system

Actually every service of radiotherapy uses a treatment planning system (TPS) to plan a simulated irradiation for external or internal beam for a patient with some cancer, the manipulation of TPS is under the responsibility of the oncologist and the medical physicists, who try to minimize the dose in healthy structures and conform the dose in the tumor [29].

The calculated algorithms, which are based the TPS, use medical imaging from the patient obtained through technical images like: computed tomography, magnetic resonance imaging and positron emission tomography [30]. Today, the modern TPS provide tools for multimodality image matching, also known as image coregistration or fusion. Different dose prediction models are available, including pencil beam, cone beam and Monte Carlo simulation, with precision versus computation time being the relevant trade-off.

The treatment simulation is used to plan the geometric and radiological aspects of the therapy using radiation. Medical physicists plan the simulation treatment based on the prescribed dose stipulated by the oncologist and the constrains of the risk organs. Thus, the TPS is used to place beams which can deliver enough radiation to a tumor trying both the criteria: minimizing the dose to healthy tissue and risk organs and deliver the prescribed dose to the tumor. For this determination many decisions are to be considered including radiation beam (that are generally photons or electrons beams), angles of radiation incidence, irradiation field, whether attenuation wedges are to be used, and which multileaf collimator configuration will be used to shape the radiation from each beam [31]. Plans are often evaluated through dose-volume histograms, that can show the uniformity of the dose to the diseased tissue (tumor) and sparing of healthy structures. The obtained plan from the TPS can be evaluated comparing it with experimental measurements and also through the one simulation code.

5. MAGIC-*f*, PENELOPE and TPS use for dosimetry in some clinical cases for electron beams

5.1. Dosimetric response of the MAGIC-*f* gel for electron beams

Polymer gel dosimeters have been studied for use in dosimetry for photon beams for the characteristics of high spatial resolution and determination of dose in three-dimensional dose distributions. Some properties like response dependence on dose, energy and dose rate are not well established for electron beams.

The objective of this work is to evaluate the use of MAGIC-*f* gel dosimeter for electron beam in radiotherapy.

5.1.1. Materials and methods

Samples of MAGIC-*f* gel were manufactured following the protocols establish by Fernandes [15] and poured into three cylindrical glass tubes routinely used for blood sample collection (BD Vacutainer®) with 5ml volume, 12mm diameter for a specific measurement. Experimental irradiations were made at Hospital de Câncer de Barretos (HCB), using a Varian 2100c linear accelerator.

Variation of dose-response from Magic-*f* gel was evaluated verifying the possibility of the linear behavior of the gel for two energies, 9 and 15 MeV at a dose range of 1 to 10 Gy. To evaluate the response the dose rate were varied from 80cGy/min to 400cGy. The assessment of the response of the dosimeter in different depth was performed through the percentage depth dose (PDD) for the same energy with a irradiation field of 15 x 15 cm^2 at 100 cm from the water.

The readings of the gel samples were performed with the relaxometry technique in tomography mode of nuclear resonance magnetic (NMR), Philips 3.0 Tesla, from the section of Radiological from Hospital Clinic. The acquisition sequence of the NMR images were made with the multi spin-echo with 5 echoes, time echo of 20ms, repetition time and 0,250m spatial resolution. Figure 1 shows the NMR images and their maps of R2.

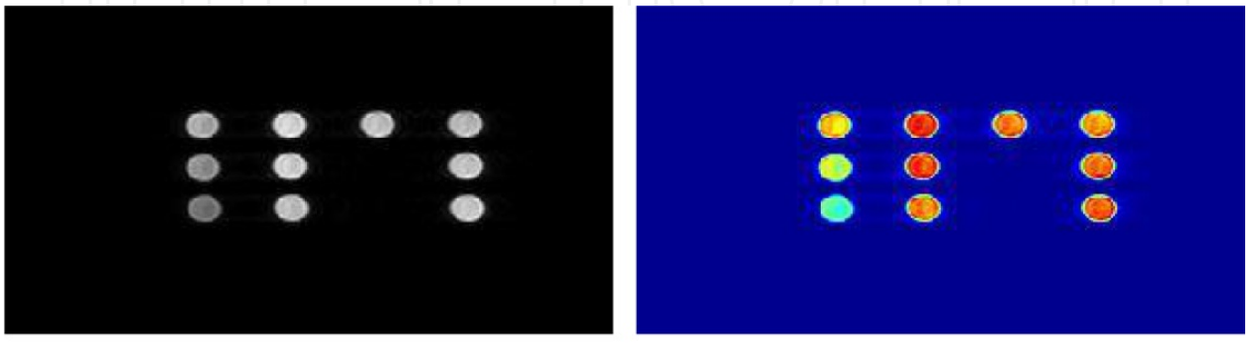

(a) (b)

Figure 1. Images of the axial section of the phantom: (a) NMR images; (b) R2 maps.

Figure 2 shows NMR images of relaxometry and R2 map normalized corresponding to the dose maps, when can be determine the PDD.

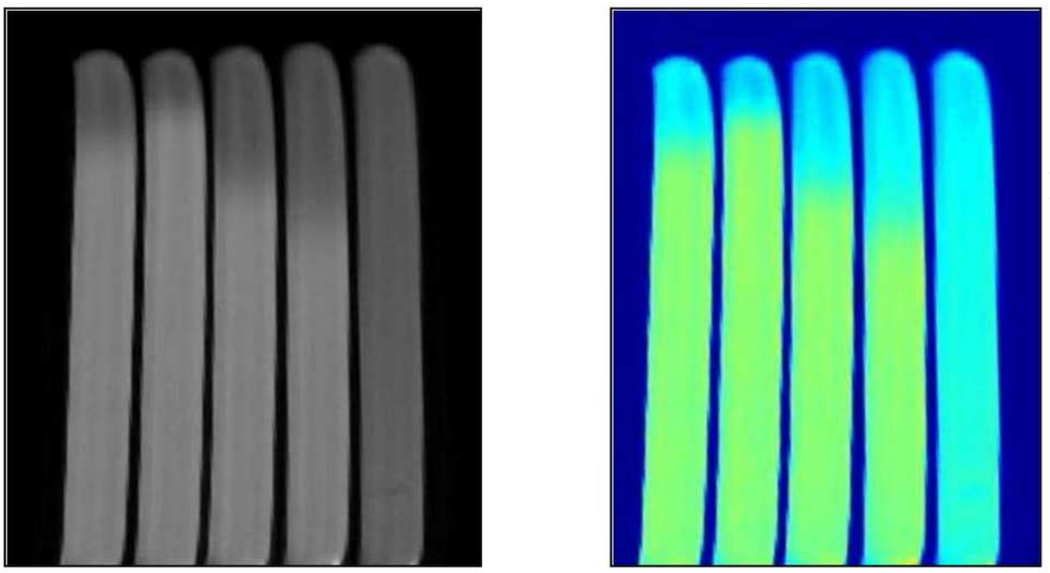

(a) (b)

Figure 2. Phantom to determine the PDD: (a) RNM image and (b) R2 maps.

5.1.2. Results and discussions

The irradiation with different dose rates have different degrees of polymerization, which can be visualized by the difference in tone of the phantoms irradiated, so that Figure 3 shows this difference of polymerization.

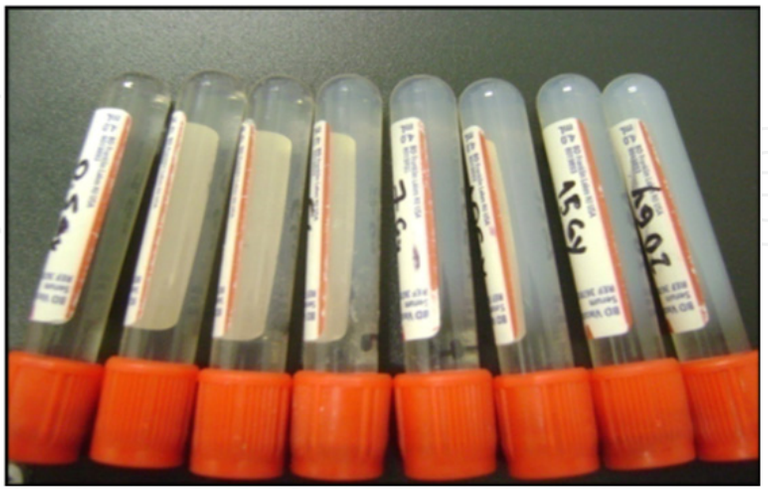

Figure 3. MAGIC-*f* irradiated with different doses.

The results obtained from the evaluation of Magic-*f* gel with the variation of the dose and dose rate are shown in figure 4.

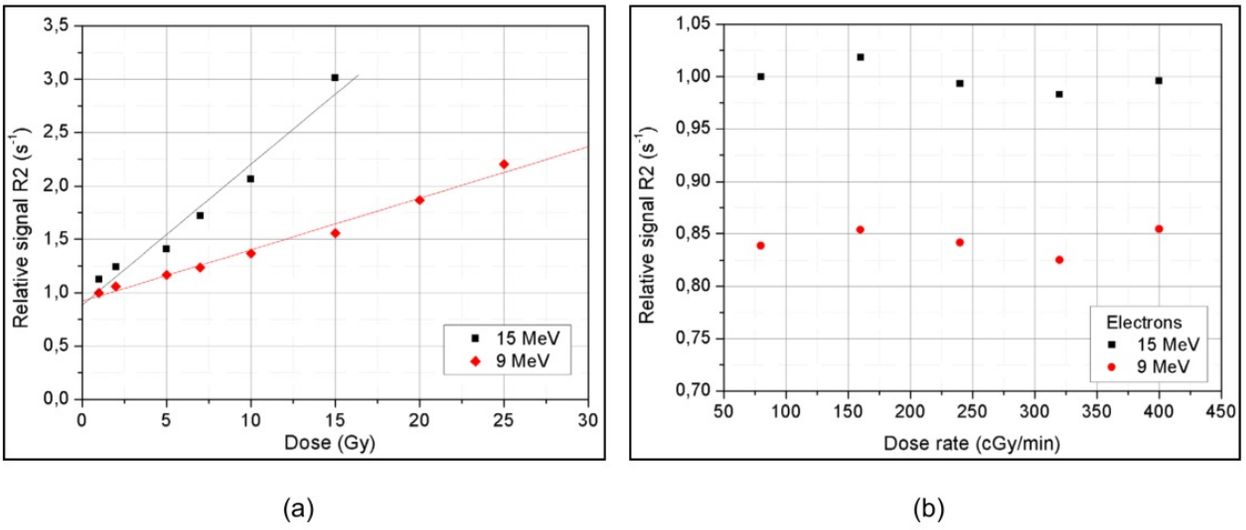

Figure 4. MAGIC-f response to energies of 9 and 15 MeV: (a) variation in dose and, (b) variation in dose rate.

For all measurements the maximum uncertainty of 1.8% was found, from signal average of each irradiated homogeneous region. This was calculated through the mean of three acquisition images for each measurement.

From figure 4 (a) it can be observed that Magic-*f* gel show a dependence to different energies, with a high variation of 50% when the signal R2 from both energies to the absorbed dose of 15 Gy is compared. The linearity of the curves show correlation coefficient, r2, 0,9819 e 0,9916 for energies of 9 and 15 MeV, respectively.

The curve of the rate dose-response of the gel, shown in figure 4 (b), and the linearity curves the in figure 4 (a) show the dose dependence of the gel and maximum variations of 1.7% and 3.4% were found for energies of 9 and 15 MeV, respectively.

Figure 5 shows the phantoms irradiated for determination of PDD curves. PDD curves obtained with the gel are shown in figure 6, which were compared with the PDD obtained through ionization chamber (ic).

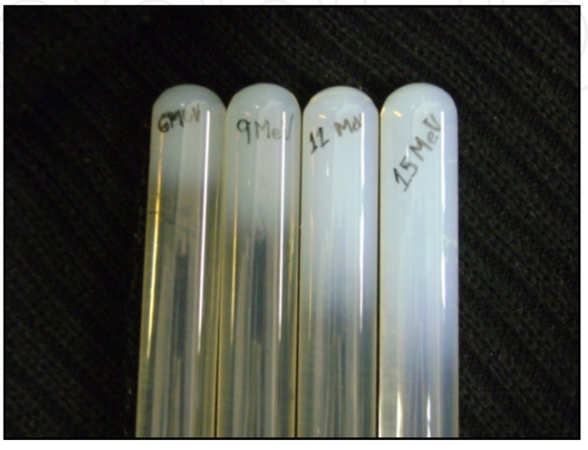

Figure 5. MAGIC-*f* irradiated with different energies.

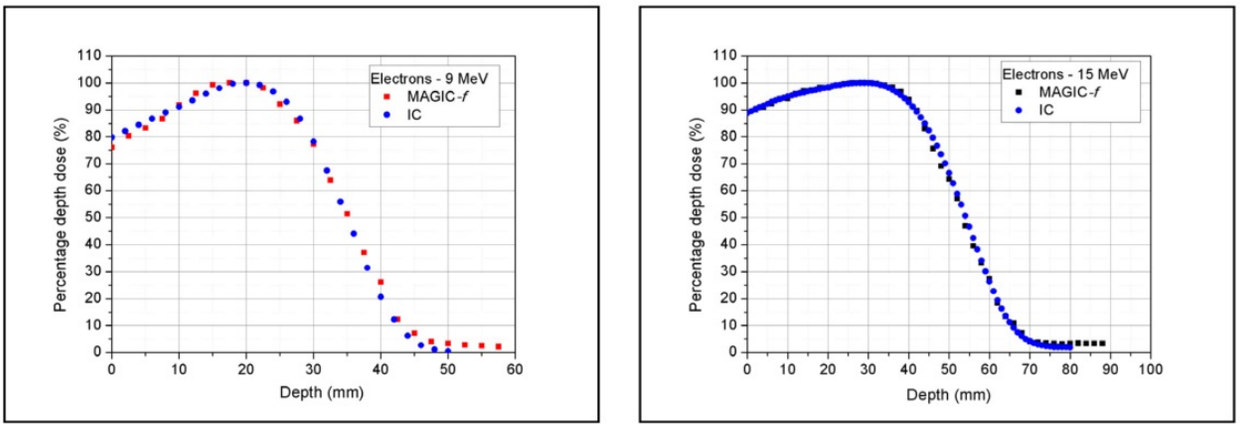

(a) (b)

Figure 6. PDD obtained with Magic-*f* gel and ionization chamber for two energies: (a) 9 MeV e (b) 15 MeV.

The maximum percentage different of 4.0% was found on comparison of PDD curves obtained with the Magic -*f* gel and ionization chamber for energies of 9 and 15 MeV.

5.1.3. Conclusion

From the results we can affirm that MAGIC-*f* dosimeter can be used as a complementary dosimetric tool for determination of the characteristics of the clinical electrons beams.

5.2. Mixed dose distribution of electron and photon beams through the gel dosimeter MAGIC-f and PENELOPE-Monte Carlo Simulation

Combining electron and photon fields in the same radiation plan can improve dose distributions, delivering a homogeneous dose to the target while reducing the dose to normal tissues. This treatment technique can benefit from both the finite range of the electrons and the sharper penumbra of the photons.

The aim of this application is to evaluate the improvement in the dose distributions from treatments using mixed photon and electron beams through polymer gel dosimetry with MAGIC-*f* and Monte Carlo simulation using PENELOPE.

5.2.1. Materials and methods

A cylindrical phantom with dimensions of 10 cm diameter and 12 cm height was homogeneously filled with MAGIC-*f*. The phantom was irradiated with a 6 MV photon beam and a 12 MeV electron beam. Field sizes of 3 x 7 cm^2 at 100 cm SSD were used to deliver a prescribed dose of 8 Gy for each beam. The phantom analysis followed a previous developed protocol in which an MRI image is registered one day after irradiation. A 3.0 T MRI scanner using a head coil and a multiple spin echo sequence with 16 echos, TE = 22.5 ms and TR = 3000 ms was used for readings. From the MRI images, R2 values were

calculated on a pixel-by-pixel basis to produce R2 maps related the absorbed dose. The same geometry used in the irradiation process was simulated by PENELOPE with spatial resolution of 1 mm. The depth doses and dose profiles were used to compare the results from experiments (MAGIC-*f*) and simulation.

5.2.2. Results and discussions

The dose distributions obtained with Monte Carlo simulation are presented in the figure 7 and the dosimetric parameters obtained with PENELOPE and MAGIC-*f* are presented in figure 8.

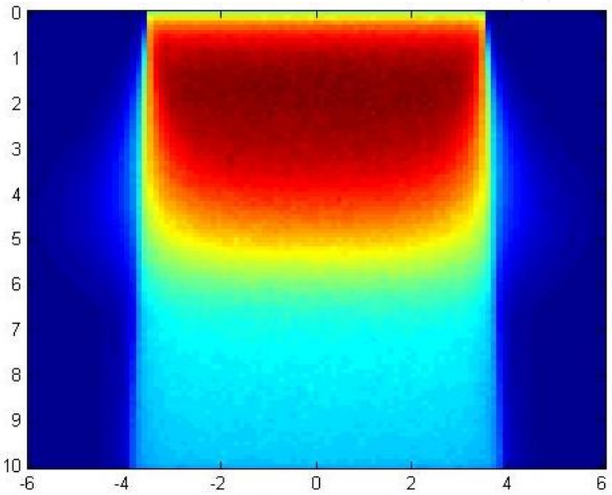

Figure 7. Dose distribution obtained with PENELOPE.

The comparisons between PENELOPE and MAGIC-*f* showed maximum differences of 3.0% and 3.2%, inside the volume of the 90% isodose for the beam profile and for the PDP curves, respectively.

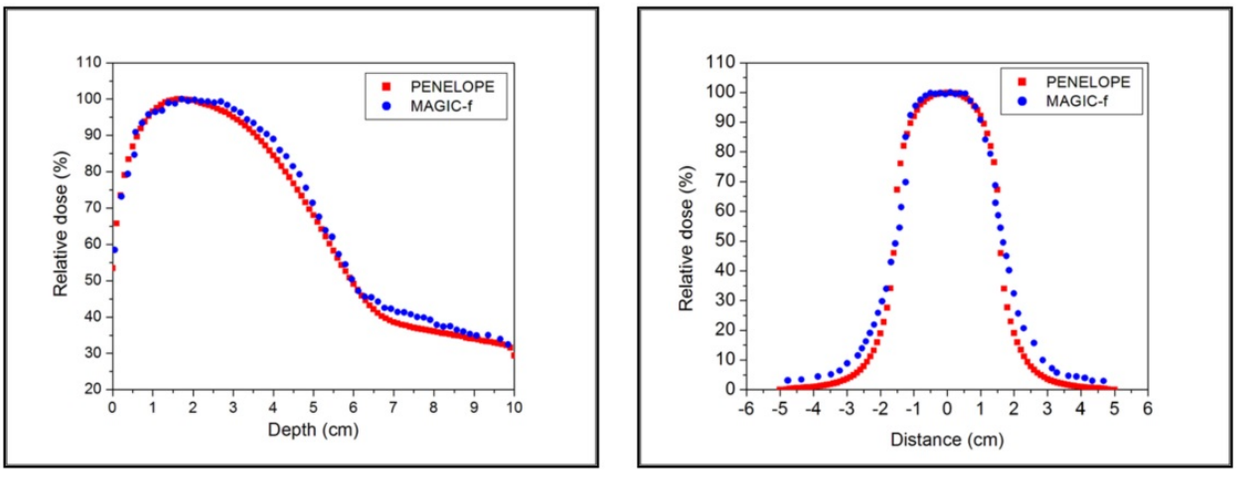

(a) (b)

Figure 8. Dosimetric parameters obtained with PENELOPE and MAGIC-f: (a) PDD; (b) beam profile.

5.2.3. Conclusions

The comparison between the dose distribution for PENELOPE and MAGIC-*f* showed that gel dosimeter can be used in radiotherapy, for special applications, as photons and electrons mixed fields. Also, the results showed that the mixed fields reduce the absorbed dose in entrance of the prescribed field, compared with the typical electron treatment.

5.3. Evaluation of collimated fields with electron beam through XiO treatment planning system and PENELOPE Monte Carlo simulation

The determination of dose distribution by system of planning and simulation codes is different mainly due to calculation algorithm. Dose distribution may vary depending upon the dosimetric parameters, for example, the field size. The PDP for collimated fields were evaluated by the XiO treatment planning system (TPS) and PENELOPE Monte Carlo simulation. Figure 9 shows the dose distribution obtained for different field size for the 9 MeV.

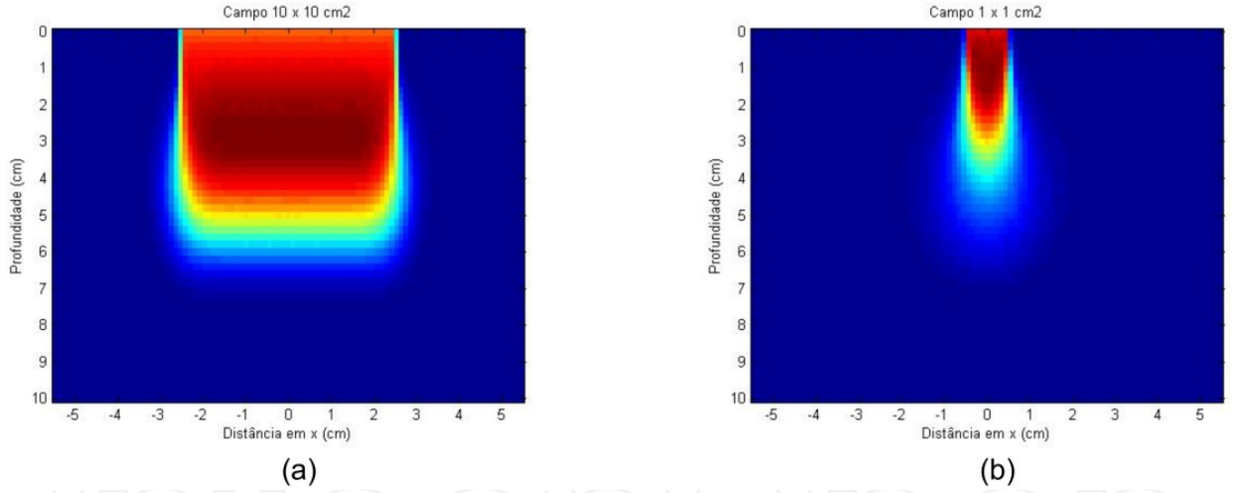

Figure 9. Dose distribution obtained for different field size for the 9: (a) 10 x 10 cm², (b) 1 x 1 cm².

5.3.1. Materials and methods

Using the standard applicators for electrons beam of 10x10 cm² beam profiles through PENELOPE, TPS and ionization chamber (0.1cc/IBA) were determined. From the concordances between the two calculation algorithm, simulation code and TPS, were studied for collimated fields. The standard applicator of 10 x 10 cm² and blocks of cerrobend were used to collimate fields of 1x1 , 3x3 and 5x5 cm², for 9 MeV beam(fig:10). The PDD obtained by the code and TPS were analyzed with the MatLab® software.

Figure 10. Cerrobend collimator.

5.3.2. Results and discussions

A maximum difference of 1.5 % when comparing the values obtained from the PENELOPE and ionization chamber for PDD obtained at the maximum depth dose and 2.2 % when TPS and ionization values were compared, for the two applicators respectively. A maximum difference of 3.0% and 3.2% were also found on comparing with other depth using PENELOPE and TPS. These differences increase to 5% for isodose less than 50 %, as shown in figure 11.

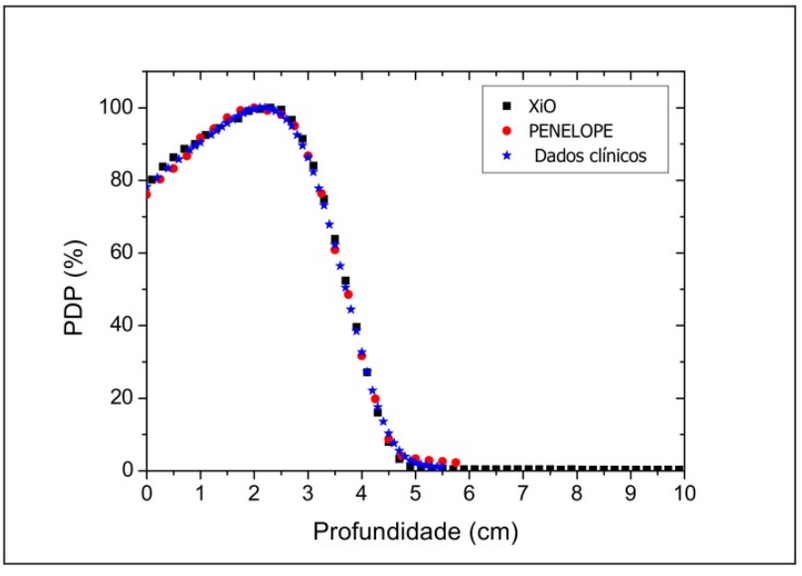

Figure 11. PDD in reference condition for dosimetric tool: XiO, PENELOPE and ionization chamber

The comparison of the PDD obtained at depth greater than 50% showed maximum difference of 5.0 %, 4.3 %, 4.8 %, respectively for each studied field. These differences increase to 12% for other depth, as shown in figure 12.

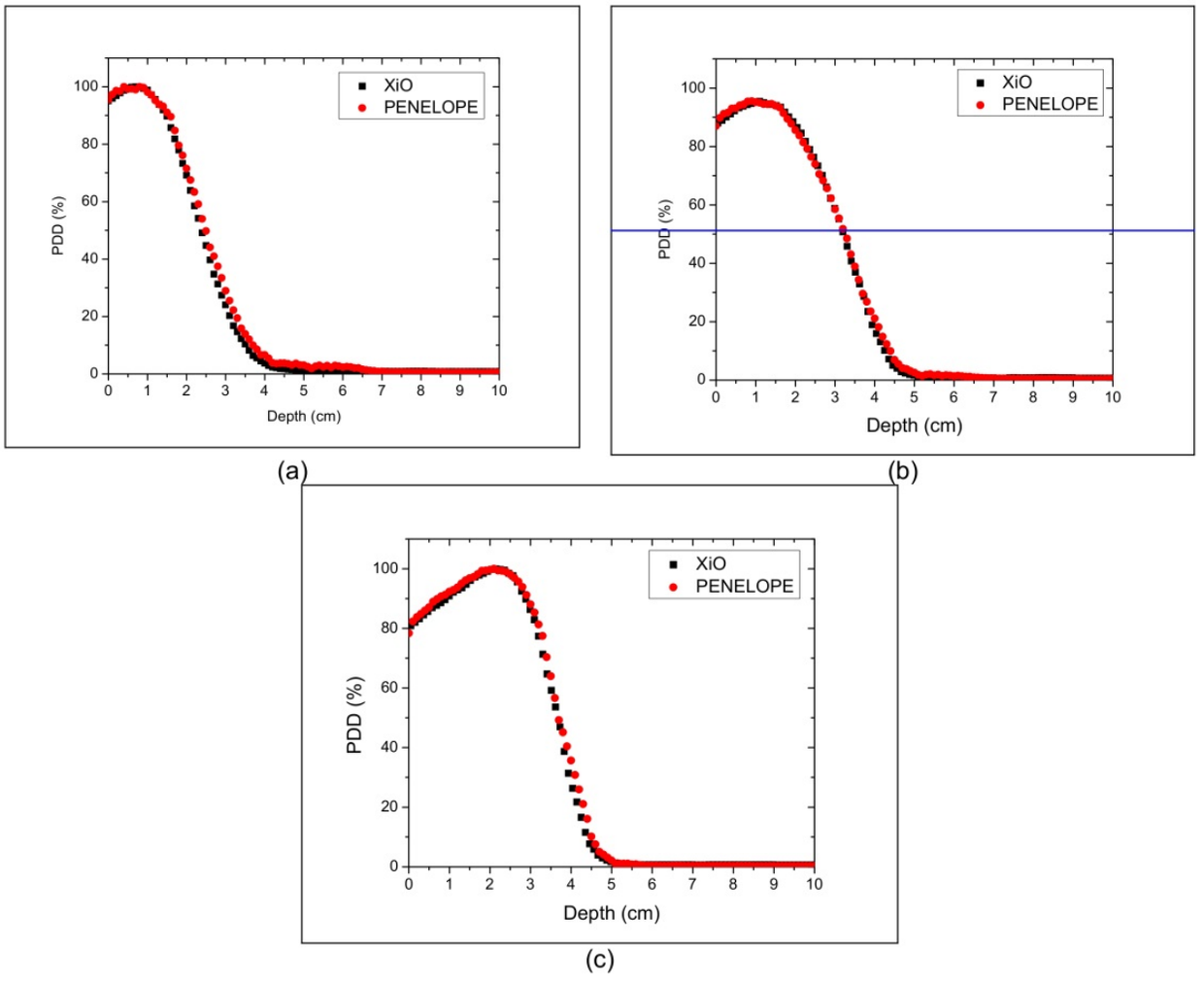

Figure 12. PDD obtained for 9 MeV in different fields size: (a) 1 x 1 cm², (b) 3 x 3 cm², (a) 5 x 5 cm².

5.3.3. Conclusion

The TPS curves did not show a continuous behavior due the interpolation of data for these collimated fields. From the results it can be inferred that despite the differences of both calculation algorithm the behavior of the beam profiles was similar.

5.4. Study of different materials for a conformational simulation in radiotherapy using the PENELOPE-Monte Carlo code

The use of conformal techniques for photons beam represent the most modern procedures in radiotherapy, like intensity modulation radiation (IMRT), the intra-operative radiotherapy (IORT) and tomotherapy. For photon beams, irregular fields are obtained through shielding blocks of high atomic number, specially manufactured for each patient, or by liear accelerator accessories such as multi-leaf collimators. Since this collimation enables better targeting of treatment of the target volume while protecting surrounding healthy tissues, the use of conformal techniques in radiotherapy with photons beams has made it

possible to increase the prescribed dose compared with those used in conventional techniques.

For electron beams, currently, the irradiation units are not fitted with suitable accessories to give a conformal technique, although with the technological progress of the radiotherapy and the improvement of the algorithms used in the treatment planning system, radiotherapy with modulated electron (MERT) beams may be a more tangible possibility. Thus, the dosimetric characteristics of the irradiation fields produced by this proposal have been investigated in this study.

Recent authors have studied different possibilities for realization of this new radiotherapy technique, An example being the construction of the multi-leaf collimators for a specific electron beam [32]. The possibility of using the multi-leaf collimators using only photon beams[33] or development of collimators additional to maintain a standard feature of the treatment with electrons beams [34,35].

However, for the modality of MERT the major limitation is the thickness of the additional collimators used because of the short distance between the applicator and irradiated surface pattern, requiring investigation of the possibility of using high atomic number materials in the manufacture of additional collimator.

Hence the additional optimization of collimators may be determined using computational simulation, which is a useful alternative to the experimental methods, it has the advantaged of providing detailed studies and in different experimental conditions without using methodologies that are time-consuming and costly [36].

The proposition of this study is to analyze using Monte Carlo simulation with the PENELOPE code to determination of dose distribution, PDD, and dose profiles obtained with the MERT technique with additional collimators of different material: cerrobend (cerr) and acrylic (PMMA)

5.4.1. Materials and methods

The different dosimetric response of collimator for the treatment of MERT were evaluated using Monte Carlo simulation with PENELOPE code, version 2008.The geometry of simulation is shown in figure 13.

In this study, we used spectra electron beam 6 and 15 MeV specific for the linear accelerator Clinac 2100 C (Varian) irradiating an object simulator of 20 x 20 x 20 cm^3 filled with water. The SSD used was 100 cm, the irradiation field of 10 x 10 cm^2, and collimated by the additional applicator for an irradiation field of 1 x 1 cm^2. PDD and the beam profile in the depth of treatment (85% isodose) were determined by PENELOPE code for both materials and energy, with spatial resolution of 1 mm along the central axis of the radiation field. Were also determined the distribution of doses deposited in planes parallel and perpendicular to the central axis of the radiation beams used.

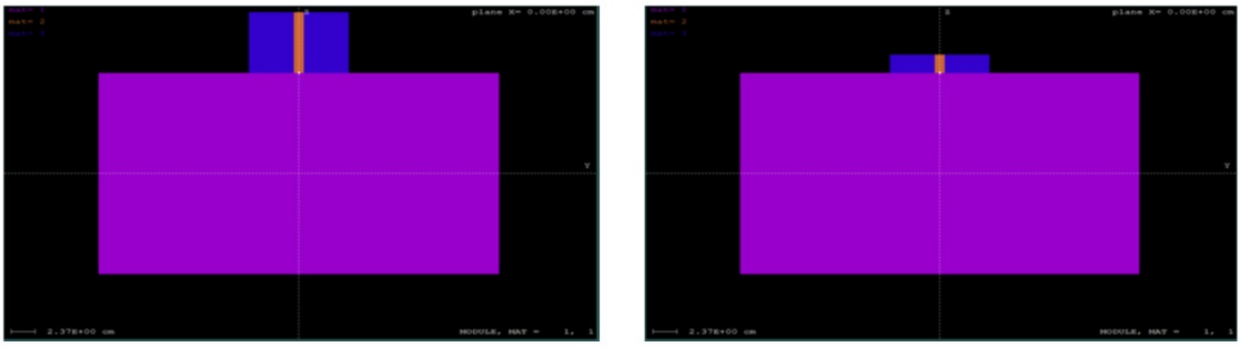

(a) (b)

Figure 13. Geometry simulated for spectrum of 6 MeV with different collimators additional: (a) PMMA and (b) Cerrobend.

The thickness of the collimators additional cerrobend and PMMA were determined using the same attenuation in different materials and different energies. Table 1 shows the thicknesses used in the simulation.

	Thickness of the additional collimator (cm)	
Energy (MeV)	Cerr	PMMA
6	1,8	6,0
15	3,3	10,9

Table 1. Thickness for both additional collimators

5.4.2. Results and discussions

The doses distribution of one plane is represented in phantom is shown in Figure 14, showing, qualitatively, the difference in dose distribution obtained for the same collimator additional material, acrylic, for both radiation beams 6 and 15MeV.

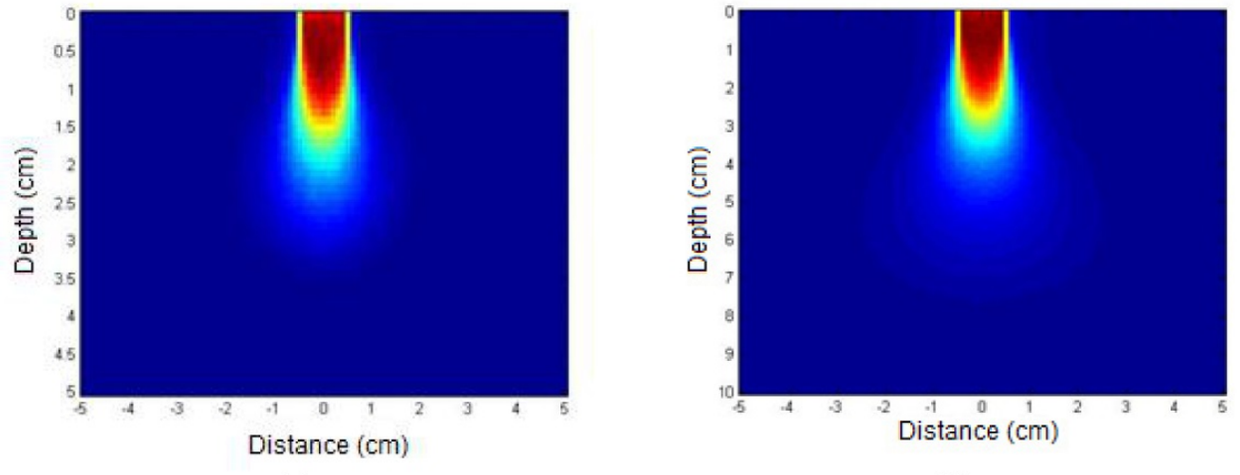

(a) (b)

Figure 14. Dose distributions with the acrylic collimator for the energies of: (a) 6 MeV, (b) 15 MeV.

The obtained dosimetric responses for different material and energies are presented in figures 15 and 16.

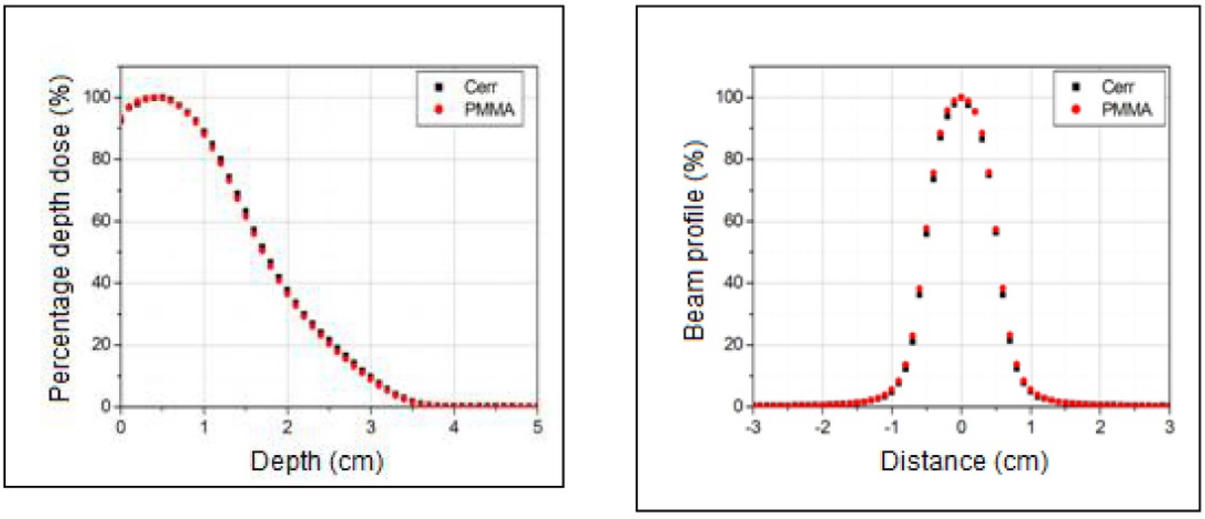

(a) (b)

Figure 15. Comparison of the two results obtained with the Cerrobend and PMMA for energies of 6 MeV: (a) PDD, (b) Beam profile.

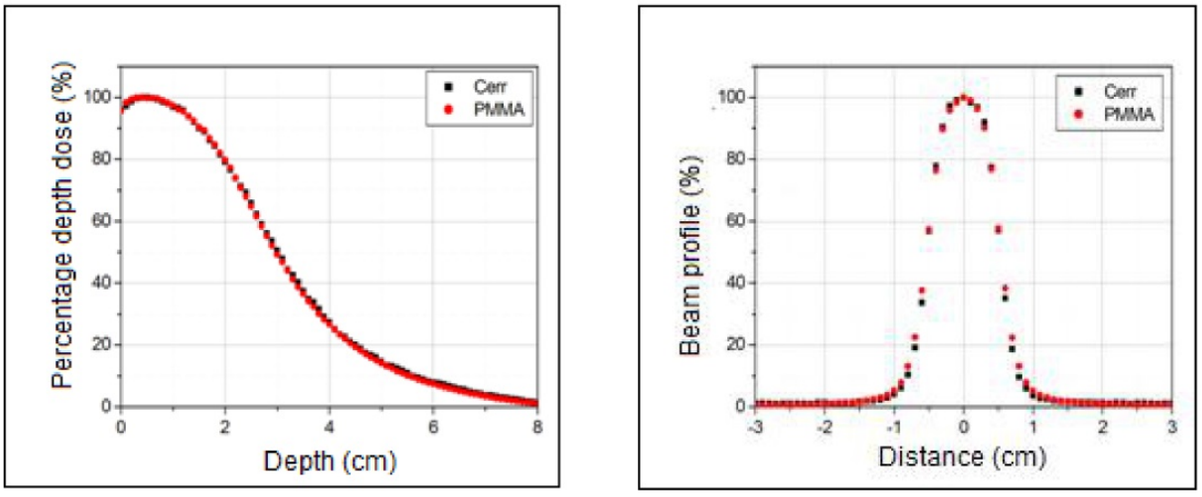

(a) (b)

Figure 16. Comparison of the two results obtained with the Cerrobend and PMMA for energies of 15 MeV: (a) PDD, (b) Beam profile.

Table 2 shows, quantitatively, the major differences from dosimetric parameters, PDD and beam profile at treatment depth, with collimators cerrobend and PMMA for energies of 6 MeV and 15 MeV

Since the irradiation characteristics of an electron beam, it was expected that there were greater photon contamination when the collimator was added a material of high atomic

number such as cerrobend, however, results presented in Figures 15 and 16 show that the thickness of the collimator is added to attenuate photons produced contamination is reduced, with the same responses observed with the material suitable for collimator of electrons, such as PMMA, with the advantage of lower thickness.

Energy (MeV)	PDD (%)	Beam Profile (%)
6	1,2	2,5
15	1,5	3,2

Table 2. Percentages of the major differences for the dosimetric parameters, were evaluated the additional collimators (cerr and PMMA) in the energies of 6 MeV and 15 MeV.

5.4.3. Conclusions

It can be inferred therefore, that the additional collimator for the proposed technique can be manufactured using a material of high atomic number, conserving dosimetric characteristics already established, with the advantage of lower thickness.

Author details

Thatiane Alves Pianoschi and Mirko Salomón Alva-Sánchez
Department of Physics, University of São Paulo, Ribeirão Preto, SP, Brazil

Acknowledgement

The presented works were supported by: CAPES (Coordination of Improvement of Higher Education Personnel- *Portuguese: Coordenação de Aperfeiçoamento de Pessoal de Nível Superior*) and the physics department of the University of Sao Paulo-Campus Ribeirao Preto-Brazil.

We are thankfully to the personnel from the Cancer Hospital of Barretos, especially to Marcelo Carvalho Santanna and Fransico Américo Marcelino. Hospital of Clinics from Ribeirão Preto, Hospital Sírio Libanês- Sao Paulo-Brazil, especially to Cecilia Hadad.

The authors are thankfully to the professor Ph. D. Patricia Nicolucci to orientation for all the works, which are part of our doctorate work.

We are thankfully for technical support to José Luiz Aziani and Carlos Renato da Silva is also appreciated.

6. References

[1] Hogstrom K, Almond P (2006) Review of electron beam therapy physics. Phys. Med. Biol. 51 R455–R489.

[2] Khan F, Doppke K, Hogstrom K (1991) Clinical electron-beam dosimetry: Report of AAPM Radiation Therapy Committee Task Group No. 25. Med. Phys. 18: 73-107.

[3] Sempau J, Fernandez-Varea J, Acosta E (2003) Experimental benchmarks of the Monte Carlo code PENELOPE. Nuc. Instrum. Methods Phys. Res. B 207:107-123.
[4] Rogers D (2006) Reviews: Fifty years of Monte Carlo simulations for medical physics, Phys. Med. Biol. 51:R287 – R301.
[5] Day M, Stein G (1950) Chemical effects of ionizing radiation in some gels. Nature. 166:141-147.
[6] Andrews H, Murphy R, LeBrun E (1957) Gel dosimeter for depth dose measurements. Rev. Sci. Instrum. 28:329-332.
[7] Gore J, Kang Y, Schulz R (1984) Measurement of radiation dose distributions by nuclear magnetic resonance (NMR) imaging. Phys. Med. Biol. 29:1189-1197.
[8] Maryanski M, Gore J, Kennan R, Schulz R (1993) NMR relaxation enhancement in gels polymerized and cross-linked by ionizing radiation: a new approach to 3D dosimeter by MRI. Mag. reson. imaging. 11: 253-258.
[9] Maryanski M, Schultz R, Ibbott G, Gatenby J, Xie J, Horton D, Gore J (1994) Magnetic resonance imaging of radiation dose distributions using a polymer-gel dosimeter. Phys. med. biol. 39: 1437-1455.
[10] Baldock C, Burford R, Billinghan N, Wagner G, Patval S, Badawi R, Keevil S (1998) Experimental procedure for the manufacture of polycrylamide gel (PAG) for magnetic resonance imaging (MRI) radiation dosimetry. Phys. med. biol. 43: 695-702.
[11] Fong P, Keil D, Does M, Gore J (2001) Polymer gels for magnetic resonance imaging of radiation dose distributions at normal room atmosphere. Phys. med. biol. 46: 3105-3113.
[12] Baldock C, Burford R, Billinghan N, Wagner G, Patval S, Badawi R, Keevil S (1998) Experimental procedure for the manufacture of polycrylamide gel (PAG) for magnetic resonance imaging (MRI) radiation dosimetry. Phys. med. biol. 43: 695-702.
[13] De Deene Y, Hurley C, Venning A, Vergote K, Mather M, Healy B, Baldock C (2002) A basic study of some normoxic polymer gel dosimeter. Phys. med. biol. 47: 3441-3463.
[14] Gustavsson H, Karlsson A, Back S, Olsson L, Haraldsson P, Engstrom P, Nystrom H (2003) MAGIC-type gel for three-dimensional dosimetry: Intensity-modulated radiation therapy verification. Med. phys. 30:1264-1271.
[15] Fernandes J, Pastorello B, de Araujo D, Baffa O (2008) Formaldehyde increases magic gel dosimeter melting point and sensitivity. Phys. med. biol. 53: N1-N6.
[16] Kramer G, Crowley P, Burns L (2000) Investigation the impossible: Monte Carlos simulation Radiat. Prot. Dosimetry. 89: 259 – 262.
[17] Bielajew A, Rogers D (1992) A standard timing benchmark for EGS4 Monte Carlo calculation Med. Phys. 19:303 – 304.
[18] Hendrikcs J, Adams K, Booth T (2001) Present and future capabilities of MCNP. App. Radiat. Isotopes. 53: 857 – 861.
[19] Salvat F, Fernández-Varea J, Sempau J (2008) A Code System for Monte-Carlo Simulation of Electron and Photon Transport France.
[20] Allison J, Amako J, Apostolakis H (2006) Geant4 developments and applications. IEEE Transactions on nuclear science. 53: 70-78.

[21] Brualla L, Palanco-Zamora R, Witting A (2009) Comparison between PENELOPE and electron Monte Carlo simulations of electron fields used in the treatment of conjunctival lymphoma Phys. Med. Biol. 54:5469-5481.
[22] Duclous R, Dubroca B, Frank M (2010) Deterministic partial differential equation model for dose calculation in electron radiotherapy. Phys. Med. Biol. 55: 3843-3857.
[23] Casado F, Garcia-Pareja S, Cenizo E (2010) Dosimetric characterization of an Ir-192 brachytherapy source with the Monte Carlo code PENELOPE. Physica Medica. 26:132-139.
[24] Sempau J, Badal A, Brualla L (2011) A PENELOPE-based system for the automated Monte Carlo simulation of clinacs and voxelized geometries—application to far-from-axis fields. Med. phys. 38: 5887-5895.
[25] Koivunoroa H, Siiskonen T, Kotiluoto P, Auterinen I, Hippelainen E, Savolainen S (2012) Accuracy of the electron transport in MCNP5 and its suitability for ionization chamber response simulations: A comparison with the EGSNRC and PENELOPE codes. Med. phys. 39:1335-1344.
[26] Ramirez J, Chen F, Nicolucci P, Baffa O (2011) Dosimetry of small radiation field in inhomogeneous medium using alanine/EPR minidosimeters and PENELOPE Monte Carlo simulation. Radiat. Measur.46:941-944.
[27] Gonzales D, Requena S, Williams S (2012) Au La x-rays induced by photons from 241Am: Comparison of experimental results and the predictions of PENELOPE. Appl. Radiat. Isot. 70: 301–304.
[28] International commission on radiation units and measurements, ICRU, (1989) Prescribing, Tissue substitutes in radiation dosimetry and measurement, ICRU Report 44, EUA.
[29] Hendee W, Ibbott G, Hendee E (2005) Radiation Therapy Physics. Wiley-Liss Publ. ISBN 0-471-39493-9.
[30] Lahanas M,Baltas D,Giannouli S (2003) Global convergence analysis of fast multiobjective gradient-based dose optimization algorithms for high-dose-rate brachytherapy. Phys. Med. Biol. 48:599-617.
[31] Galvin M, Ezzel G, Eisbrauch A, Yu C, Butler B, Xiao Y, Rosen I, Rosenman I (2004) Implementing IMRT in clinical practice: a joint document of the American Society for Therapeutic Radiology and Oncology and the American Association of Physicists in Medicine. Int. J. Radiat. Oncol. Biol. Phys. 58: 1616–34.
[32] Gauer T, Albers D, Cremers F, Harmansa R (2006) Design of a computer-controlled multileaf collimator for advanced electron radiotherapy. Phys. Med. Biol. 51: 5987-6003.
[33] Jin L, Ma M-C, Fan J (2008) Dosimetric verification of modulated electron radiotherapy delivered using a photon multileaf collimator for intact breasts. Phys. Med. Biol. 53: 6009-6025.
[34] Al-Yahya K, Verhaegen F, Seuntjens J (2007) Design and dosimetry of a few leaf electron collimators for energy modulated electron therapy. Med. Phys. 34(12): 4782-4791.
[35] Vatanen T, Traneus E, Lahtinen T (2008) Dosimetric verification of a Monte Carlo electron beam model for na add-on eMLC. Phys. Med. Biol. 53(2): 391-404.
[36] Sempau J, Acosta E, Baró J (1997) An algorithm for Monte Carlo simulation of coupled electron-photon transport, Nucl. Instr. and Meth. B. 132: 377-390.